Ca^{2+} Influx Does Not Trigger Glucose-Induced Traffic of the Insulin Granules and Alteration of Their Distribution

ICHIRO NIKI,*†[1] TAE NIWA,† WEI YU,‡ DOROTA BUDZKO,† TAKASHI MIKI,§ AND TAKAO SENDA¶

Department of Pharmacology, Oita University, Faculty of Medicine, Oita 879-5593, Japan; Departments of †Cell Pharmacology and ‡Anatomy, Nagoya University Graduate School of Medicine, Nagoya 466-8550, Japan; §Division of Molecular Medicine, Center for Biomedical Science, Chiba University School of Medicine, Chiba 260-8670, Japan; and ¶Department of Anatomy I, Fujita Health University School of Medicine, Toyoake 470-1192, Japan

This study investigated mechanisms by which glucose increases readily releasable secretory granules *via* acting on preexocytotic steps, i.e., intracellular granule movement and granule access to the plasma membrane using a pancreatic β-cell line, MIN6. Glucose-induced activation of the movement occurred at a substimulatory concentration with regard to insulin output. Glucose activation of the movement was inhibited by pretreatment with thapsigargin plus acetylcholine to suppress intracellular Ca^{2+} mobilization. Inhibitors of calmodulin and myosin light chain kinase also suppressed glucose activation of the movement. Simultaneous addition of glucose with Ca^{2+} channel blockers or the ATP-sensitive K^+ channel opener diazoxide failed to suppress the traffic activation, and addition of these substances on top of glucose stimulation resulted in a further increase. Although stimulatory glucose had minimal changes in the intracellular granule distribution, inhibition of Ca^{2+} influx revealed increases by glucose of the granules in the cell periphery. In contrast, high K^+ depolarization decreased the peripheral granules. Glucose-induced granule margination was abolished when the protein kinase C activity was downregulated. These findings indicate that preexocytotic control of insulin release is regulated by distinct mechanisms from Ca^{2+} influx, which triggers insulin exocytosis. The nature of the regulation by glucose may explain a part of potentiating effects of the hexose independent of the closure of the ATP-sensitive K^+ channel. Exp Biol Med 228:1218–1226, 2003

Key words: pancreatic β-cell; granule mobilization; granule docking; myosin; novel protein kinase C

Elevation of blood glucose levels causes release of insulin, the most important hormone for the strict control of glucose homeostasis. Disorder of the secretory response of the pancreatic β-cell has been considered to be one of the causes of Type II diabetes mellitus (1, 2). The mechanism by which the hexose sugar controls insulin release is complex. Ca^{2+} influx, which is essential for exocytosis of insulin granules, is achieved by membrane depolarization due to closure of the ATP-sensitive K^+ channel (K_{ATP}) by increased ATP as a result of glucose metabolism, and eventual opening of the voltage-dependent Ca^{2+} channel (3). K_{ATP}-dependent Ca^{2+} influx is the determinant of insulin exocytosis, the final stage of the β-cell secretory events, which was recently confirmed by gene knockout of the pore-forming subunit of the K_{ATP}, Kir6.2 (4).

Glucose, however, exerts versatile roles in the β-cell secretory machinery at the exocytotic stage and some proximal steps as well. Translocation of the secretory granules is a preexocytotic step in the secretory cascade that plays an important role in the regulation of hormone output (5). We have investigated regulation of the intracellular movement of the secretory granules in living pancreatic β-cells by a bioimaging approach and demonstrated that glucose exerts a stimulating effect (6), which reconfirms an early report with cinemicrography (7).

Before released to the extracellular space, the granules need to be docked to the plasma membrane. We have recently attempted to quantify insulin granules distributed in the vicinity of the plasma membrane by immunostaining with anti-insulin antibody, and we demonstrated that activation of protein kinase C (PKC) may be required for the insulin granules to be distributed in the cell periphery (8).

In this study, we examined the intracellular messenger system underlying the transduction of the glucose signal in insulin granule traffic in the cytoplasm and their access to

This work was supported in part by Grants-in-Aid for Research from the Ministry of Education, Science, Sports and Culture, Japan.

[1] To whom requests for reprints should be addressed at Department of Pharmacology, Oita University, Faculty of Medicine, 1-1 Idaigaoka, Hasama, Oita 879-5593, Japan. E-mail: niki@med.iota-u.ac.jp

1535-3702/03/22810-1218$15.00

the plasma membrane, both of which turned out not to be triggered by Ca^{2+} influx.

Materials and Methods

Materials. D-glucose, 12-O-tetradecanoyl-phorbol 13-acetate (TPA), nitrendipine, and thapsigargin were purchased from Wako (Tokyo, Japan). Dulbecco's modified Eagles medium (DMEM) was from Nissui (Tokyo, Japan). Glibenclamide, mannoheptulose, 2-deoxyglucose, iodoacetate, p-nitrophenyl-α-D-glucopyranoside (α-PNP-Glu), diazoxide, acetylcholine, and monoclonal antibody against myosin light chain (MLC) were from Sigma (St. Louis, MO). Nifedipine was from Fujisawa Pharmaceutical Co. (Osaka, Japan). Glass-bottom tissue culture dishes (35 mm in diameter) were from Meridian Instruments Far East (Tokyo, Japan). Guinea pig anti-insulin antibody was from Seikagaku Kogyo (Tokyo, Japan). Rhodamine-conjugated goat anti-guinea pig IgG was from ICN (Costa Mesa, CA). The calmodulin antagonist W-7 (N-(6-aminohexyl)-5-chloro-1-naphthalene-sulfonamide) and its less active analogue W-5 (N-(6-aminohexyl)-1-naphthalene-sulfonamide), the specific inhibitor of myosin light chain kinase (MLCK), ML-9 (1-(5-chloronaphthalene-sulfonyl)-1-H-hexahydro-1,4-diazepine) (9), and ML-5 (1-(naphthalene-sulfonyl)-1-H-hexahydro-1,4-diazepine), a structurally related negative control compound of ML-9 (10), were provided by Dr. H. Hidaka (D. Western Therapeutics Institute, Nagoya, Japan). The radioimmunoassay insulin kit employed was from Eiken (Tokyo, Japan). Enhanced chemiluminescence (ECL) reagents were from Amersham Japan (Tokyo).

Cell Culture. MIN6 cells were cultured in DMEM supplemented with 66 mg/l kanamycin sulfate and 15% fetal calf serum at 37°C in a humidified atmosphere of 95% air/5% CO_2 (11). The cells were passaged and harvested using trypsin/EDTA and the culture medium was replaced every other day.

Video Microscopy. Experiments were carried out with an inverted light microscope (Axiovert 135, Carl Zeiss, Germany) equipped with a ×63 objective lens (Plan-Neofluar, Carl Zeiss) and a ×2.5 insertion lens. In our observation, the granule movement was not preferentially directed to the cell periphery. The average speed of the movement was 0.8–1.0 μm/sec in MIN6 cells, which is comparable to that for another β-cell line, HIT T15 (6). Images were detected with a charge-coupled device camera (DXC-930, Sony, Japan), displayed on a monitor screen (PVM-9040, Sony), and recorded using a video tape recorder (SVO-260, Sony). Pictures were reproduced from videotape and analyzed on the monitor using an image analyser (Argus-20, Hamamatsu Photonics, Hamamatsu, Japan). The depth of the focal plane was 3–4 μm, which is one-third to one-fourth of the cell height. All these experiments were carried out at 37°C.

Quantification of Movement of the Secretory Granules. MIN6 cells were seeded at a density of 3.5–5 × 10^5 cells onto a glass-bottom culture dish (35 mm in diameter) 1–2 days prior to each experiment. On the day of experimentation, cells were preincubated at 37°C for 60 min in 1 ml of Hepes-buffered Krebs solution containing (m*M*): NaCl 119, KCl 4.75, $NaHCO_3$ 5, $CaCl_2$ 2.54, $MgSO_4$ 1.2, and Hepes 20 (pH 7.4 with NaOH), with 5 mg/ml bovine serum albumin (BSA) and then further incubated in 1 ml of Hepes-buffered Krebs solution containing 5 mg/ml BSA and various substances. In some experiments, the cells were treated with various substances as described prior to the glucose challenge. Movement of insulin granules in MIN6 cells was quantitatively assessed by the method originally devised by Lacy *et al.* (7) with some modification (6). Briefly, numbers of the granules that moved into or out of squares (3.5 × 3.5 μm) during a 30-sec period were counted. One MIN6 cell was equivalent to five or six complete squares. Statistical significance between values before and after the addition was evaluated by paired Student *t* test. More than five cells were observed for each condition, and data were expressed as the mean ± SEM of the frequency assessed in *n* squares.

Separation of Endogenous Phosphorylated MLC in MIN6 Cells. MIN6 cells (approx. 1.5 × 10^7) were incubated in 6-cm dishes for 60 min in glucose-free Hepes-buffered Krebs-Ringer solution supplemented with 5 mg/ml BSA. After washing twice, the cells were further incubated for 15 min in Hepes-buffered Krebs-Ringer solution (see above) with or without glucose. Separation of phosphorylated MLC was carried out according to Persechini *et al.* (12) with some modification (13). Briefly, after addition of 5% trichloroacetic acid (TCA) and 2 m*M* dithiothreitol (DTT) (final concentrations), the cells were left for 10 min at room temperature and scraped from the dishes. The extracts were centrifuged and washed with acetone containing 10 m*M* DTT four times in a glass tube and pellets were dissolved in 100-μl urea sample buffer (8.3 *M* urea, 20 m*M* Tris-base, 22 m*M* glycine, 10 m*M* DTT, and 0.1% bromophenol blue). Proteins (~10 μg) were separated on a polyacrylamide gel (15% polyacrylamide, 0.75% bisacrylamide, 40% glycerol, 20 m*M* Tris-base, and 23 m*M* glycine) at 450 V for 3 hr, transferred onto nitrocellulose membranes, and exposed to anti-MLC antibody. The phosphorylated forms of MLC migrate faster than the nonphosphorylated form because of differences in viscosity or sedimentation coefficients (12). The density of each immunopositive band, visualized with the ECL kit, was determined densitometrically, and the extent of MLC phosphorylation was expressed as the percentage of the total (non-plus monophosphorylated) MLC in each lane.

Immunofluorescence Microscopy. Granule access to the plasma membrane was assessed by examining intracellular distribution of the insulin granules by fluorescent immunostaining with anti-insulin antibody (8). MIN6 cells attached onto glass cover slips placed in 12-well culture plates were washed three times with 5 mg/ml BSA-containing Hepes-buffered Krebs buffer and preincubated in the identical buffer for 1 hr. The cells were then incubated

under various conditions for 1 hr. For downregulation of the PKC activity, the cells were treated overnight with 200 n*M* TPA in the culture medium prior to glucose-free preincubation. After washing with phosphate-buffered saline (PBS), they were fixed with 4% paraformaldehyde for 15 min and subsequently with 99.5% ethanol for 5 min at room temperature. The cells were then incubated with guinea pig anti-insulin antibody. The cells were further washed with PBS and incubated in rhodamine-conjugated goat anti-guinea pig IgG for 1 hr. After washing, the cells were mounted in a drop of 90% glycerol/PBS containing 0.1% phenylenediamine as an antifade and observed using a fluorescent microscope (E-800, Nikon, Tokyo, Japan) equipped with confocal laser scanning system (MR-1024, Japan Bio-Rad, Tokyo, Japan). More than 200 cells in each condition were observed in one experiment. The pattern was then classified into three categories: insulin granules distributed evenly throughout the cytoplasm without their accumulation at the cell periphery (cytoplasmic pattern); insulin granules distributed throughout the cytoplasm with their moderate accumulation at the cell periphery (intermediate pattern); and insulin granules highly accumulated at the cell periphery (peripheral pattern). Any treatment employed here did not cause obvious changes of the cell shape. Data are expressed as mean ± SE values from three to five independent experiments. The granule margination was defined as significant changes of the rate for the peripheral pattern versus those for the cytoplasmic and intermediate patterns by the χ^2 test.

Insulin Assay. MIN6 cells were seeded at a density of 1×10^5 cells per well in 24-well tissue culture plates 3–4 days prior to each experiment. On the day of experimentation, cells were reincubated at 37°C for 1 hr in 1 ml of Hepes-buffered Krebs solution with 5 mg/ml BSA without glucose. To deplete the cells of the PKC activity, the cells were pretreated with TPA as described above. Cells were further incubated for 1 hr in 1 ml of the same solution containing 5 mg/ml BSA under various conditions. For TPA-downregulated cells, samples were taken every 20 min in the following 1-hr incubation. An aliquot was collected, centrifuged briefly to sediment any detached cells, and stored at –20°C until assayed. Insulin released into the medium was measured by radioimmunoassay using bovine insulin as a standard. In our preliminary experiments, we found that the glucose-free preincubation did not affect glucose-induced insulin secretion. Values were expressed as the mean ± SEM and statistical significance was assessed with the unpaired Student *t* test.

Results

Dose-Dependent Effects of Glucose on Granule Movement and Insulin Release in MIN6 Cells. Figure 1A illustrates a dose-dependent increase by glucose of insulin release from MIN6 cells. Glucose increased insulin release with a threshold concentration between 3 and 10 m*M*. The threshold concentration of glucose for secretion was similar to that observed in normal mouse islet preparation (14), though the amplitude was rather small in this cell line (five- to six-fold increase under maximal stimulation). Effects of increasing concentrations of glucose on the movement of insulin granules in MIN6 cells are demonstrated in Figure 1B. On sequential observation of nonstimulated cells, a gradual decrease (20%–30%) in the movement occurred over a 20-min observation period partly because we experience that long exposure to an intense light slows down the granule movement. Glucose increased intracellular movement of the insulin granules in a dose-dependent manner, and activation of the movement required lower concentrations of glucose than that for insulin release. The movement was increased by the addition of glucose which was followed by a gradual decrease thereafter.

Effects of a Sweet Taste Inhibitor and Metabolic Inhibitors on Insulin Release and Intracellular Movement of Insulin Granules. Findings for inhibition of glucose-induced insulin release by metabolic inhibitors and a sweet sense inhibitor are shown in Table I. Mannoheptulose and 2-deoxyglucose at 20 m*M* were equally effective at inhibiting glucose-induced insulin release from MIN6 cells. Inhibition by mannoheptulose was, however, less than in normal islet cells (15). In contrast, the sweet taste inhibitor, α-PNP-Glu, was more effective at suppressing glucose-induced insulin release from MIN6 cells than that from normal islets (16). Iodoacetate (1 m*M*), which influences glucose metabolism by inhibiting glyceraldehyde-3-phosphate dehydrogenase (15), demonstrated the most potent suppression of glucose-induced insulin release.

These metabolic inhibitors and the sweet taste inhibitor also caused suppression of the granule movement with different potencies. 2-Deoxyglucose partially inhibited the glucose-induced movement, whereas mannoheptulose almost nullified the glucose effect. Iodoacetate suppressed granule movement by glucose potently. With regard to inhibition of movement, α-PNP-Glu was the most potent among those tested here.

Glucose-Induced Activation of Granule Movement and Influence of Various Compounds That Influence Ca^{2+} Signaling. We investigated effects of pharmacological agents acting on Ca^{2+} signaling on intracellular movement of insulin granules (Table II). Neither of the two dihydropyridine Ca^{2+} channel blockers (nifedipine and nitrendipine) caused significant inhibition of the granule movement, whereas these compounds at concentrations used here suppressed glucose-induced insulin release (with 20 m*M* glucose plus 2 μ*M* nifedipine and 0.3 μ*M* nitrendipine, 23.0% ± 2.7% and 28.2% ± 2.3% of insulin release by 20 m*M* glucose alone, respectively). Glucose-induced movement of the insulin granules was also increased in the co-presence of the K_{ATP} opener, diazoxide at 100 μ*M*, which potently suppressed glucose-induced insulin secretion (with 100 μ*M* diazoxide and 20 m*M* glucose, 26.1% ± 6.7% of insulin release by 20 m*M* glucose occurred). Negative involvement of Ca^{2+} influx in the control of the move-

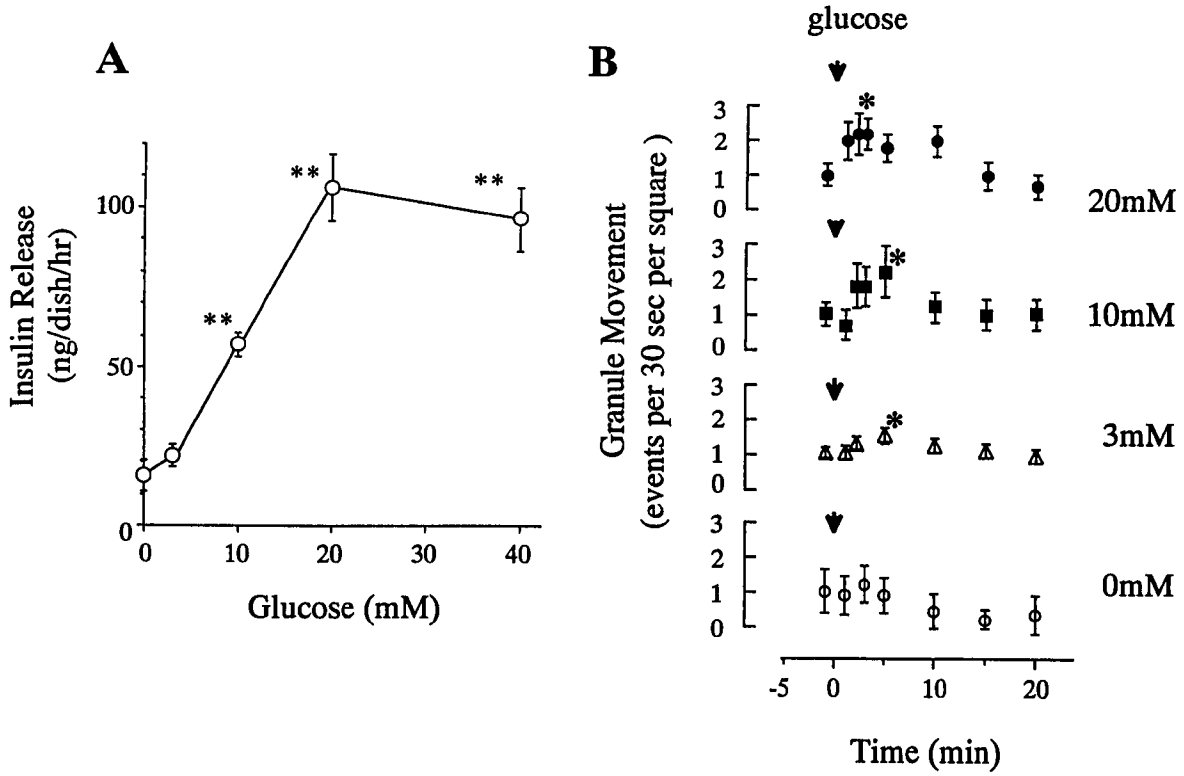

Figure 1. Dose-dependent effects of glucose on insulin release from and movement of insulin granules in MIN6 cells. (A) MIN6 cells (0.1×10^5 cells/well) were seeded onto 24-well plates 2–3 days prior to the experiments. On the day of experimentation, the cells were preincubated for 1 hr in the absence of glucose and further incubated for 1 hr with various concentrations of glucose. At the end of the incubation, the medium was collected for insulin assay. Each symbol represents the mean ± SEM for 4 observations. $^{**}P < 0.01$ estimated by unpaired *t* test. (B) MIN6 cells were seeded onto glass-bottom plastic dishes. After 1-hr incubation in glucose-free buffer, the cells were stimulated by increasing concentrations of glucose as described and intracellular movement of the insulin granules was observed by phase-contrast microscopy. The frequency of the granule movement was worked out by counting the number of the granules that go out of or come into a 3.5 × 3.5 square during 30 sec. Each symbol represents the mean ± SEM for observations of 30–32 squares. $^{*}P < 0.05$ estimated by the paired *t* test.

Table I. Effects of Metabolic Inhibitors and a Sweet Taste Inhibitor on Insulin Release and Intracellular Movement of the Insulin Granules in MIN6 Cells

	Insulin release (*n*) (percentage of control)	Granule movement (events per 30 sec per square)				
		Glucose (20 m*M*) challenge		Percentage of change	*n*	*P*
		Before	After			
Glucose (20 m*M*)	100 ± 7.3 (5)	2.13 ± 0.19	3.03 ± 0.24	+42.3	32	<0.001
+ α-PNP-Glu (20 m*M*)	15.1 ± 1.8 (5)	1.96 ± 0.23	0.64 ± 0.16	−67.3	28	<0.001
+ manoheptulose (20 m*M*)	62.0 ± 2.9 (5)	1.67 ± 0.23	1.63 ± 0.22	−2.4	43	n.s.
+ 2-deoxyglucose (20 m*M*)	60.8 ± 6.7 (5)	1.52 ± 0.15	1.81 ± 0.20	+19.1	54	n.s.
+ iodoacetate (1 m*M*)	4.1 ± 0.2 (5)	1.85 ± 0.16	1.34 ± 0.15	−27.6	59	<0.05

Note. Insulin secretion: MIN6 cells (0.1×10^5 cells/well) were seeded onto 24-well plates 2 to 3 days before the experiments. On the day of experimentation, the cells were preincubated for 1 hr under glucose-free conditions, and were then further incubated for 1 hr in a medium containing 20 m*M* glucose and various metabolic inhibitor described above. At the end of the incubation, the medium was collected for insulin assay. Each value represents the mean ± SEM when expressed as percentage of glucose (20 m*M*)-induced insulin release. Granule movement: Secretory granules in living MIN6 cells were observed by phase-contrast microscopy. Movement was assessed 2 min before and 5 min after addition of the substances plus glucose. Statistical significance between before and after values was assessed by paired *t* test.

ment was confirmed by addition of these Ca^{2+} channel blockers or diazoxide after glucose activation. As shown in Figure 2A–C, all these compounds further increased the traffic frequency when added 4 min after glucose addition. These compounds alone did not have any effects on the traffic (data not shown). Glibenclamide (1 μ*M*), an antidiabetic sulfonylurea, which causes closure of K_{ATP} and eventual Ca^{2+} influx, increased insulin release from MIN6 cells (625.9% ± 59.4% of the basal release, $n = 5$). The compound, however, failed to activate granule movement (2.31 ± 0.25 at 2 min before and 2.38 ± 0.32 at 5 min after the addition of glibenclamide, $n = 16$). These results are com-

Table II. Effects of Various Inhibitors on Glucose-Induced Activation of Granule Traffic in MIN6 Cells

Additions	Granule movement (events per 30 sec per square)				
	Glucose (20 m*M*) challenge		Percentage of change	*n*	*P*
	Before	After			
None (20 m*M* glucose only)	2.13 ± 0.19	3.03 ± 0.24	+42.3	32	<0.001
Nifedipine (2 μ*M*)[a]	1.93 ± 0.19	2.40 ± 0.21	+25.7	30	<0.01
Nitrendipine (0.3 μ*M*)[a]	1.54 ± 0.26	2.15 ± 0.25	+39.6	26	<0.05
Diazoxide (100 μ*M*)[a]	1.54 ± 0.34	2.89 ± 0.35	+87.6	28	<0.001
Acetylcholine (100 μ*M*) + thapsigargin (1 μ*M*)[b]	1.18 ± 0.27	1.07 ± 0.21	−9.4	27	n.s.
W-7 (10 μ*M*)[b]	2.17 ± 0.19	1.97 ± 0.23	−9.3	29	n.s.
W-5 (10 μ*M*)[b]	2.43 ± 0.22	2.87 ± 0.23	+18.1	30	<0.05
ML-9 (30 μ*M*)[b]	2.01 ± 0.21	2.10 ± 0.21	+4.5	29	n.s.
ML-5 (30 μ*M*)[b]	2.52 ± 0.18	2.93 ± 0.22	+16.3	29	<0.05

Note. Insulin granules in living MIN6 cells were observed by phase-contrast microscopy and video recorded, and numbers of granules that moved into or out of squares (3.5 × 3.5 μm) were counted for 30 sec.
[a] Nifedipine, nitrendipine, and diazoxide were added to the medium simultaneously with 20 m*M* glucose.
[b] Inhibitors were added 10 min before the glucose challenge. Intracellular movement of insulin granules was analyzed 2 min before and 5 min after the glucose addition. Data are mean ± SEM values for the numbers of squares indicated in the *n* column. Statistical significance was assessed by paired *t* test.

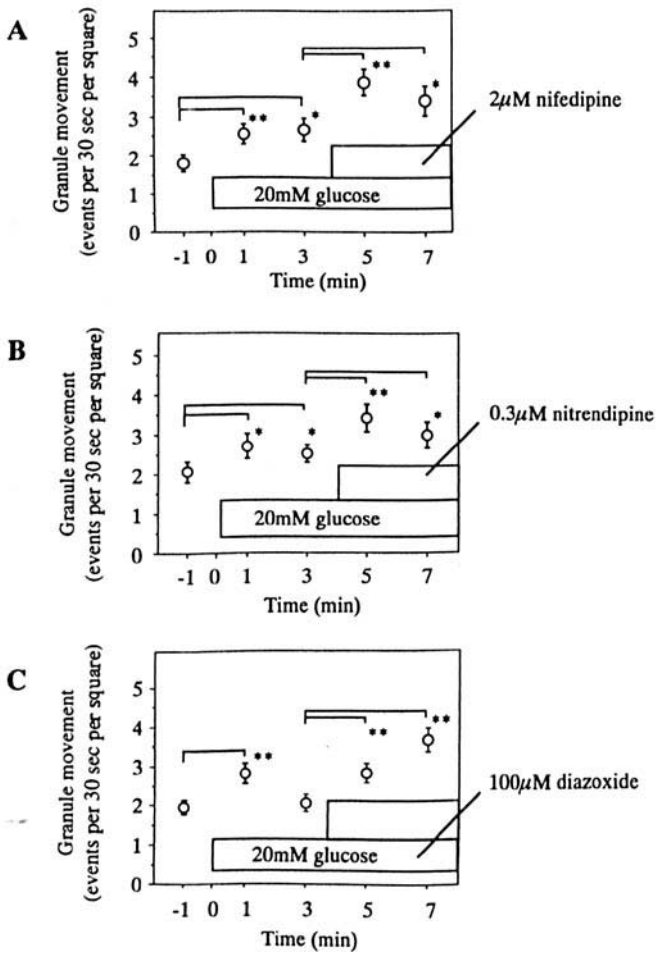

Figure 2. Effects of Ca^{2+} channel blockers and diazoxide on glucose-stimulated insulin granule movement in the MIN6 pancreatic β-cells. After 1 hr incubation in glucose-free Hepes-Krebs buffer, the cells were stimulated by 20 m*M* glucose followed by addition of nifedipine (A), nitrendipine (B), and diazoxide (C) at 3, 0.3, and 100 μ*M*, respectively. Intracellular movement of the insulin granules was observed by phase-contrast microscopy. Each symbol represents the mean ± SEM for 44–62 squares. $^*P < 0.05$, and $^{**}P < 0.005$ when estimated by the paired *t* test.

patible with findings that tolbutamide, another antidiabetic sulfonylurea, or depolarizing K^+ did not increase intracellular traffic of the insulin granules (6, 17). The calmodulin inhibitor W-7 inhibited the movement of intracellular granules under basal conditions (data not shown) and also suppressed glucose activation. The MLCK inhibitor ML-9, which inhibits glucose-induced insulin release (18), also caused a significant decrease in the basal movement (not shown) and nullified the effect of glucose. In contrast, the structurally related and less active control compounds for W-7 and ML-9, W-5 and ML-5, respectively, caused smaller changes in the basal movement (not shown) and failed to inhibit the activation of movement by following glucose stimulation.

Endogenous Phosphorylation of MLC in MIN6 Cells. The proportion of monophosphorylated MLC under basal conditions was variable (10%–40%) among the experiments when estimated densitometrically. However, incubation of MIN6 cells with glucose at 20 and 40 m*M* consistently increased the rate of monophosphorylated form (for Fig. 3, from 13.3% [basal] to 21.3% and 29.5% with 20 m*M* and 40 m*M* glucose, respectively). A significant increase in the phosphorylated form was detected at only

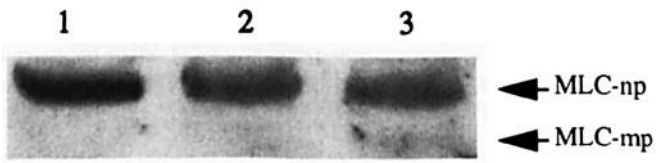

Figure 3. Endogenous phosphorylation of MLC by glucose. MIN6 cells (1×10^7 cells per sample) were incubated with 0 m*M* (lane 1), 20 m*M* (lane 2), or 40 m*M* glucose (lane 3) for 15 min. The endogenous proteins were extracted with trichloroacetic acid, denatured by urea, and loaded onto a polyacrylamide gel. Separated MLC forms were visualized by Western blotting using monoclonal anti-MLC antibody and an ECL kit. MLC-np, nonphosphorylated MLC; MLC-mp, monophosphorylated MLC. This represents 3 independent experiments with similar results.

rather high concentrations of glucose, presumably because of high activity of myosin phosphatase in the β-cell (13, 17). Diphosphorylated MLC was not detected even after glucose stimulation.

Effects of glucose on intracellular distribution of the insulin granules. We studied intracellular distribution of the insulin granules to examine effects of glucose and various substances on granule margination by estimating changes of the distribution patterns between the cytoplasmic plus intermediate groups and the peripheral one. As shown in Figure 4, a substimulatory (3 m*M*) or stimulatory (20 m*M*) concentration of glucose had minimal effects on the granule distribution. However, co-presence of nitrendipine at 1 μ*M* revealed effects of glucose (20 m*M*) that increased the peripheral granules (from 22.1% ± 1.2% for 20 m*M* glucose alone to 36.6% ± 1.4% for 20 m*M* glucose plus 1 μ*M* nitrendipine). Such changes in granule distribution were also observed with stimulatory glucose plus 100 μ*M* diazoxide (to 39.8% ± 1.8%), whereas diazoxide did not change the distribution with nonstimulatory glucose (data not shown). Depolarization of the plasma membrane with 20 m*M* K^+ increased the intermediate pattern but significantly decreased the peripheral one (14.9% ± 1.6%). In the time-dependent observation up to 60 min, 20 m*M* glucose alone had no effect on the granule margination except for 30 min after the glucose challenge. The revealing effect of diazoxide appeared 10 min after glucose stimulation and remained for the following 50 min, whereas decreasing effects of depolarizing K^+ emerged earlier (Fig. 5). When the cells were depleted of the PKC activity by overnight incubation with 200 n*M* TPA, neither nitrendipine nor diazoxide with high glucose influenced the granule distribution (Fig. 6).

Insulin Secretion From TPA-Downregulated MIN6 Cells. Figure 7 shows effects of TPA downregulation on insulin secretion from MIN6 cells. When these cells were depleted of the PKC activity, 20 m*M* glucose-induced insulin secretion was not much affected for the first 20 min. However, insulin release with 20 m*M* glucose was significantly suppressed for the next 40 min (20–40 min and 40–60 min) without changing the basal release with 3 m*M* glucose. In 1-hr batch incubation, no difference was observed in glucose-induced insulin release from MIN6 cells with or without TPA pretreatment (not shown).

Discussion

These findings demonstrate that glucose acts on preexocytotic steps in the insulin secretion cascade *via* mechanisms distinct from that for insulin exocytosis, which is triggered by Ca^{2+} influx. Previously, we first suggested that glucose activated the insulin granule movement independently of Ca^{2+} influx or K_{ATP} closure (6), but the precise mechanism was unknown. The present results with Ca^{2+} channel blockers and diazoxide as well as abolishment of glucose-induced granule traffic by pretreatment with acetylcholine and thapsigargin imply that glucose-activated movement may depend on intracellular Ca^{2+} mobilization rather than Ca^{2+} influx, which agrees with our previous

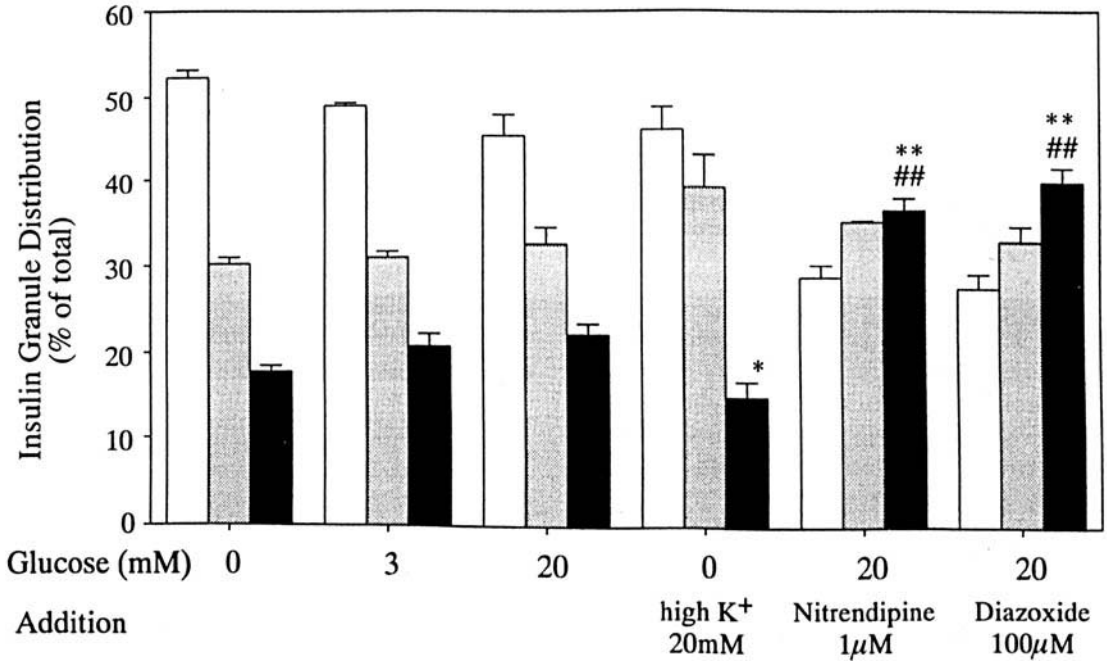

Figure 4. Changes in the intracellular distribution patterns of the insulin granules in MIN6 cells. MIN6 cells were incubated for 1 hr under various conditions, fixed, and immunostained with anti-insulin antibody. Patterns of intracellular localization of insulin immunoreactivity were classified into the 3 groups: cytoplasmic (open columns), intermediate (shaded columns), and peripheral patterns (black columns). In one experiment, more than 200 cells were observed. Statistical significance of the changes between the peripheral group and the other 2 groups was assessed by the χ^2 test. Data are expressed as the mean ± SEM of values expressed as % of total from 3–5 independent experiments. $^*P < 0.05$, $^{**}P < 0.001$ as compared with values without glucose, and $\#P < 0.05$, $\#\#P < 0.001$ as compared with those with 20 m*M* glucose alone.

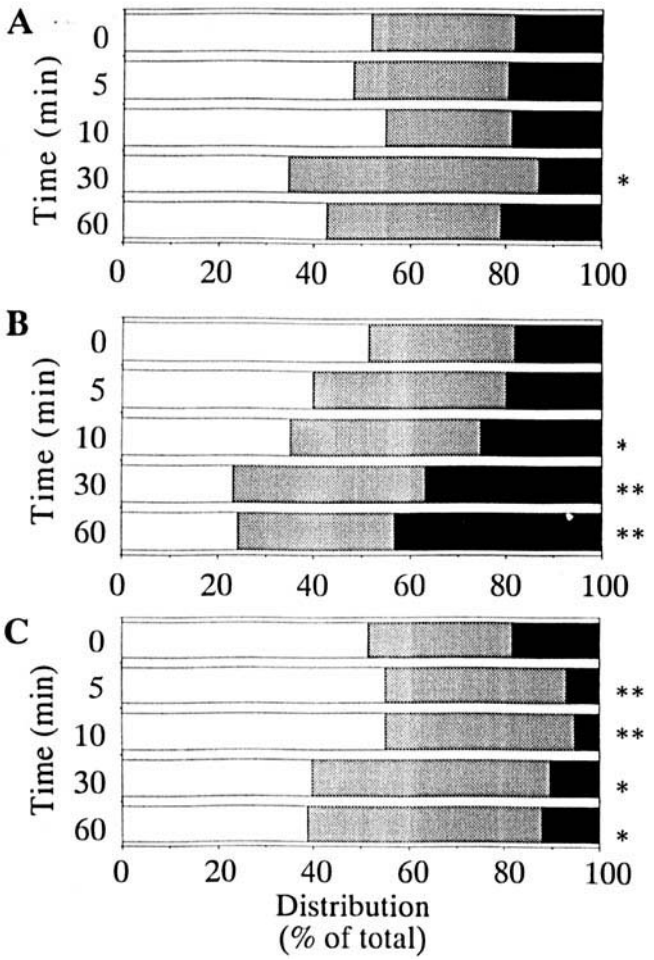

Figure 5. Time-dependent changes of the granule distribution. After glucose-free preincubation for 1 hr, MIN6 cells were incubated for 5–60 min with 20 m*M* glucose (A), 20 m*M* glucose plus 100 μ*M* diazoxide (B), and 20 m*M* KCl (C). The cells were then immunostained with anti-insulin antibody, and percentages of the granule distribution patterns were worked out as described in the text (open bars, cytoplasmic; shaded bars, intermediate; and black bars, peripheral). Data are expressed by percentages of the total cells counted. This is from 2 independent experiments with more than 400 MIN6 cells. $^{*}P < 0.05$, $^{**}P < 0.001$ as compared with those at time 0 by the χ^2 test.

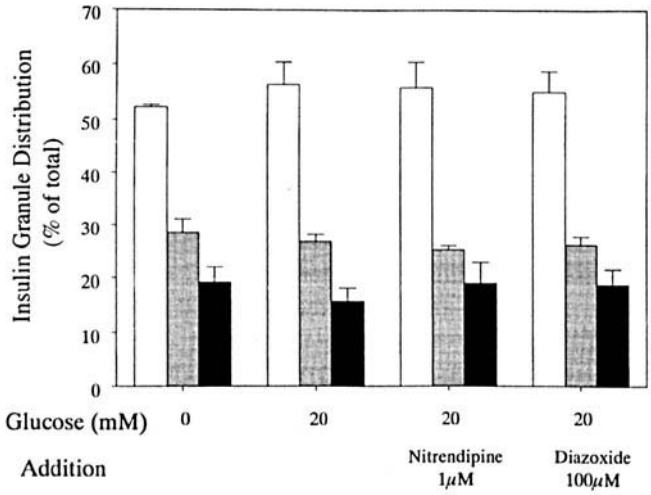

Figure 6. Intracellular distribution of the insulin granules in TPA-downregulated MIN6 cells. MIN6 cells were pretreated overnight with 200 n*M* TPA. On the day of experimentation, these cells were incubated for 1 hr in a glucose-free condition, followed by a 1-hr incubation with glucose with or without substances as described. After immunostaining with anti-insulin antibody, patterns of the granule distribution were classified. Open, shaded, and black columns represent cytoplasmic, intermediate, and peripheral types, respectively. Data are expressed as the mean ± SEM of values expressed as % of total from 3 independent experiments.

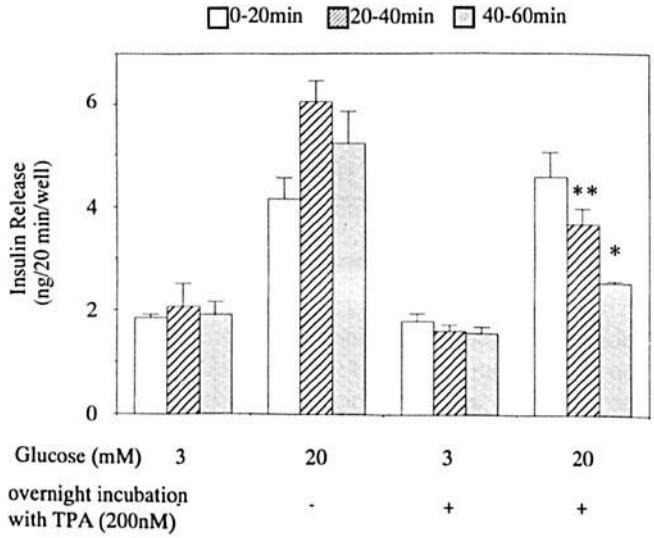

Figure 7. Glucose-induced insulin release from TPA-downregulated MIN6 β-cells. MIN6 cells (2×10^4 cells per well) were treated overnight with 200 n*M* TPA. On the day of experimentation, the cells were preincubated with glucose-free Hepes-Krebs buffer for 1 hr. The cells were then incubated with either 3 or 20 m*M* glucose as indicated. Samples were taken every 20 min, and insulin released into the medium was measured. Data are the mean ± SE for 6 observations. $^{*}P < 0.01$, $^{**}P < 0.001$ as compared with values under parallel conditions without TPA pretreatment assessed by the unpaired *t* test.

observation (17). Inhibition of glucose-induced traffic by W-7 or ML-9 suggests that Ca^{2+}/calmodulin-dependent phosphorylation of MLC may be involved in glucose activation of the movement, although the inhibition by W-7 may partly result from its inhibitory effect on Ca^{2+} mobilization as shown in another β-cell line, RIN m5F (20). This is also supported by the fact that stimulatory glucose increased phosphorylation of endogenous MLC (Fig. 3). These findings suggest that glucose and acetylcholine share a similar mechanism for activation of the granule traffic (17).

Because inositol 1,4,5-triphosphate-dependent Ca^{2+} mobilization is reported to be not potent even by stimulatory glucose in mouse β-cells, from which MIN6 cells originate (21), another mechanism may mediate glucose activation of the movement. This might result from MLC phosphorylating activity in the β-cell, which does not require the presence of functional Ca^{2+} (13). Another possibility is glucose-induced cAMP production (22), which also activates the granule traffic (6, 23). ATP-dependent activation of another motor protein kinesin may be another target (24), although direct evidence for kinesin-dependent activation by glucose has not been demonstrated. The movement was further in-

creased by inhibiting Ca^{2+} influx when added after glucose stimulation (Fig. 2), possibly because inhibition of Ca^{2+} influx prevented loss of the granules moving in the cytoplasm by suppression of insulin exocytosis.

Granule margination is another preexocytotic event of the insulin secretory cascade (5). Stimulatory glucose did not have obvious effects on the distribution, which is at variance with the recent report that docked granules in β-TC cells, estimated by immunoprecipitation with antisyntaxin antibody, were dramatically reduced by a brief exposure to glucose (25). This may be explained by differences in experimental approaches employed or by different nature of granule turnover between β-TC cells and MIN6 cells; insulin exocytosis from the readily releasable pool may be more vigorous or granule recruitment may be poorer in β-TC cells. Decreases in the peripheral granules by high K^+ may result from loss of granules by insulin exocytosis without granule refilling, because high K^+ depolarization does not increase the granule movement in MIN6 cells (17).

Interestingly, co-presence of nitrendipine or diazoxide with stimulatory glucose activated the granule margination, which implies that glucose promotes interaction between the granules and the plasma membrane. We consider that such redistribution was dismissed by glucose alone, because accumulated granules in the readily releasable pool may be lost by exocytosis under glucose stimulation. We have recently demonstrated that activation of TPA-sensitive PKC causes granule access towards the plasma membrane (8). In the β-cell, PKC has been reported to be translocated by glucose stimulation (26). These reports and the present results that glucose plus nitrendipine or diazoxide failed to influence insulin granule distribution in TPA-pretreated cells suggest implication of this kinase in the regulation of spacial redistribution of the insulin granules by glucose. The relevant substrate, however, remains to be elucidated.

Chronic exposure to TPA, which has been reported to suppress expression of the α and ε isoforms of PKC in β-cells (27), did not affect insulin release by glucose for the first 20 min, but the treatment decreased glucose-induced insulin release thereafter. This is in good agreement with the present results from the distribution study (Fig. 5), where it took 10 min until the glucose effect appeared. The TPA-sensitive PKC effect on glucose-induced redistribution of the insulin granules did not require Ca^{2+} influx, suggesting involvement of novel isoform(s) of PKC (5). Participation of PKC in the sustained, but not acute, phase of insulin release has also been suggested in other experimental systems (28, 29). Acute insulin output by glucose may be achieved from insulin granules already located in the vicinity of the plasma membrane (30).

Because glucose-induced Ca^{2+} influx into the β-cell is achieved by closure of K_{ATP} by its metabolite ATP, the glucose effects on granule movement and margination may be recognized as parts of K_{ATP}-independent actions of the hexose. The K_{ATP}-independent action, first identified as a potentiating effect of glucose even under full activation of the channel by diazoxide (31), seems to be composed of multiple effects of the hexose (32), whereas the nature of the underlying mechanism has not been entirely understood (33). Pharmacological characterization of the K_{ATP}-independent action in the previous reports suggests that the glucose effect is to some extent similar to its effects on the preexocytotic steps. For example, the K_{ATP}-independent action was suppressed by a PKC inhibitor (staurosporine) and α-PNP-Glu (32). In the previous study, protein kinases A and C were suggested to be irrelevant to the K_{ATP}-independent action, because neither forskolin nor TPA fully mimicked glucose potentiation under full activation of K_{ATP} by diazoxide, and because the K_{ATP}-independent effect remained even after chronic exposure to TPA (34). Nevertheless, it should be noted that forskolin or TPA did have small potentiating effects even with diazoxide and high K^+ (34). Because forskolin and TPA act synergistically to increase insulin release (8), these two kinases may participate in the K_{ATP}-independent actions in a distinct and cooperative manner. K_{ATP}-independent insulin release was unaffected by chronic exposure to TPA in their report, possibly because that was evaluated only by a 1-hr batch incubation.

Apart from closure of K_{ATP}, ATP may be essential for preexocytotic control of insulin release by glucose. For granule movement, ATP is necessary for MLC phosphorylation, generation of driving force *via* ATP hydrolysis by actomyosin ATPase activity, and replenishment of Ca^{2+} into the intracellular Ca^{2+} stores *via* Ca^{2+}-ATPase (13). ATP is also necessary for protein phosphorylation by PKC to promote granule margination. Such multiple roles of ATP in the preexocytotic control might be a reason why the intracellular ATP concentration or ATP/ADP ratio was well correlated with the magnitude of the K_{ATP}-independent action (33).

The authors thank Prof. Susumu Seino (Chiba University) for his helpful suggestion.

1. Leahy JL. Natural history of β-cell function in NIDDM. Diabetes Care **13**:992–1010, 1990.
2. Kahn SE. Clinical review 135: The importance of beta-cell failure in the development and progression of type 2 diabetes. J Clin Endocrinol Metab **86**:4047–4058, 2001.
3. Miki T, Nagashima K, Seino S. The structure and function of the ATP-sensitive K^+ channel in insulin-secreting pancreatic beta-cells. J Mol Endocrinol **22**:113–123, 1999.
4. Miki T, Nagashima K, Tashiro F, Kotake K, Yoshitomi H, Tamamoto A, Gonoi T, Iwanaga T, Miyazaki J-I, *et al.* Defective insulin secretion and enhanced insulin action in K_{ATP} cannel-deficient mice. Proc Natl Acad Sci U S A **95**:10402–10406, 1998.
5. Niki I, Senda T. Regulation of insulin release at pre-exocytotic stages of the secretory machinery. Curr Med Chem **2**:219–231, 2002.
6. Hisatomi M, Hidaka H, Niki I. Ca^{2+}/calmodulin and cAMP control movement of secretory granules through protein phosphorylation/dephosphorylation in the pancreatic β cell. Endocrinology **137**:4644–4649, 1996.
7. Lacy PE, Finke EH, Codilla RC. Cinemicrographic studies on β gran-

ule movement in monolayer culture of islet cells. Lab Invest **33**:570–576, 1975.
8. Yu W, Niwa T, Fukasawa T, Hidaka H, Senda T, Sasaki Y, Niki I. Synergism of protein kinases A, C and myosin light chain kinase in the secretory cascade of the pancreatic beta-cell. Diabetes **49**:945–952, 2000.
9. Ono-Saito N, Niki I, Hidaka H. H-series protein kinase inhibitors and a case of a H-series inhibitor for clinical application. Pharmacol Ther **82**:123–131, 1999.
10. Watanabe H, Takahashi R, Zhang X-X, Goto Y, Hayashi H, Ando J, Isshiki M, Seto M, Hidaka H, Niki I, Ohno R. An essential role of myosin light-chain kinase in the regulation of agonist- and fluid-flow-stimulated Ca^{2+} influx in endothelial cells. FASEB J **12**:341–348, 1998.
11. Miyazaki J, Araki K, Yamato E, Ikegami H, Asano T, Shibasaki Y, Oka Y, Yamamura K. Establishment of a pancreatic β cell line that retains glucose-inducible insulin secretion: special reference to expression of glucose transporter isoforms. Endocrinology **127**:126–132, 1990.
12. Persechini A, Kamm KE, Stull JT. Different phosphorylated forms of myosin in contracting tracheal smooth muscle. J Biol Chem **269**:6149–6152, 1994.
13. Iida Y, Senda T, Matsukawa Y, Onoda K, Miyazaki J-I, Sakaguchi H, Nimura Y, Hidaka H, Niki I. Myosin light chain phosphorylation controls insulin secretion at a proximal step in the secretory cascade. Am J Physiol **273**:E782–E789, 1997.
14. Gembal M, Gilon P, Henquin J-C. Evidence that glucose can control insulin release independently from its action on ATP-sensitive K^+ channels in mouse B cells. J Clin Invest **89**:1288–1295, 1992.
15. Zawalich WS, Pagliara AS, Matschinsky FM. Effects of iodoacetate, mannoheptulose and 3-O-methyl glucose on the secretory function and metabolism of isolated pancreatic islets. Endocrinology **100**:1276–1283, 1978.
16. Niki A, Niki H, Hashioka T. An inhibitor of sweet taste response inhibits glucose-induced insulin release. Biomed Res **10**:169–172, 1989.
17. Niwa T, Matsukawa Y, Senda T, Nimura Y, Hidaka H, Niki I. Acetylcholine activates intracellular movement of insulin granules in the pancreatic β-cells via IP_3-dependent mobilization of intracellular Ca^{2+}. Diabetes **47**:1699–1706, 1998.
18. Niki I, Okazaki K, Saitoh M, Niki A, Niki H, Tamagawa T, Iguchi A, Hidaka H. Presence and possible involvement of Ca/calmodulin-dependent protein kinases in insulin release from the rat pancreatic β cell. Biochem Biophys Res Commun **191**:255–261, 1993.
19. Niki I. Ca^{2+} signalling and secretory cascade in the pancreatic beta-cell. Jpn J Pharmacol **80**:191–197, 1999.
20. Tang SH, Yaney GC, Sharp GW. Unusual carbachol responses in RINm5F cells: evidence for a "distal" site of action in stimulus-secretion coupling. Mol Pharmacol **47**:863–870, 1995.
21. Zawalich WS, Zawalich KC. Regulation of insulin secretion by phospholipase C. Am J Physiol **271**:E401–E416, 1996.
22. Sharp GWG. The adenylate cyclase-cyclic AMP system in islets of Langerhans and its role in the control of insulin release. Diabetologia **16**:287–296, 1979.
23. Renström E, Eliasson L, Rorsman P. Protein kinase A-dependent and -independent stimulation of exocytosis by cAMP in mouse pancreatic B-cells. J Physiol **502**:105–113, 1997.
24. Varadi A, Ainscow EK, Allan VJ, Rutter GA. Involvement of conventional kinesin in glucose-stimulated secretory granule movements and exocytosis in clonal pancreatic beta-cells. J Cell Sci **115**:4177–4189, 2002.
25. Daniel S, Noda M, Straub SG, Sharp GW. Identification of the docked granule pool responsible for the first phase of glucose-stimulated insulin secretion. Diabetes **48**:1686–1690, 1999.
26. Deeney JT, Cunningham BA, Chheda S, Bokvist K, Juntti-Berggren L, Lam K, Korchak HM, Corkey BE, Berggren PO. Reversible Ca^{2+}-dependent translocation of protein kinase C and glucose-induced insulin release. J Biol Chem **271**:18154–18160, 1996.
27. Tian YM, Urquidi V, Ashcroft SJ. Protein kinase C in beta-cells: Expression of multiple isoforms and involvement in cholinergic stimulation of insulin secretion. Mol Cell Endocrinol **119**:185–193, 1996.
28. Thams P, Capito K, Hedeskov CJ, Kofod H. Phorbol-ester-induced down-regulation of protein kinase C in mouse pancreatic islets: Potentiation of phase 1 and inhibition of phase 2 of glucose-induced insulin secretion. Biochem J **265**:777–787, 1990.
29. Persaud SJ, Jones PM, Howell SL. Activation of protein kinase C is essential for sustained insulin secretion in response to cholinergic stimulation. Biochim Biophys Acta **1091**:120–122, 1991.
30. Eliasson L, Renström E, Ding W-G, Proks P, Rorsman P. Rapid ATP-dependent priming of secretory granules precedes Ca^{2+}-induced exocytosis in mouse pancreatic B-cells. J Physiol **503**:399–412, 1997.
31. Sato Y, Aizawa T, Komatsu M, Okada N, Yamada T. Dual functional role of membrane depolarization/Ca^{2+} influx in rat pancreatic B-cell. Diabetes **41**:438–443, 1992.
32. Aizawa T, Sato Y, Ishihawa F, Taguchi N, Komatsu M, Suzuki N, Hashizume K, Yamada T. ATP-sensitive K^+ channel-independent glucose action in rat pancreatic β-cell. Am J Physiol **266**:C622–C627, 1994.
33. Sato Y, Henquin J-C. The K-ATP channel-independent pathway of regulation of insulin secretion by glucose: In search of the underlying mechanism. Diabetes **47**:1713–1721, 1998.
34. Gembal M, Detimary P, Gilon P, Gao Z-Y, Henquin J-C. Mechanisms by which glucose can control insulin release independently from its action on adenosine triphosphate-sensitive K^+ channels in mouse B cells. J Clin Invest **91**:871–880, 1993.